Temperature Effects on Size and Morphology Controlled NiO nanomaterials and their Electrocatalytic Activity in Methanol Oxidation Reaction

A. Catherine Swetha[a] and Arumugam Murugadoss[*b]

[1]Department of Inorganic Chemistry, University of Madras, Guindy Campus, Chennai 600 025, Tamil Nadu, India.

[*]Corresponding author: ammuruga@gmail.com, murugadoss@unom.ac.in

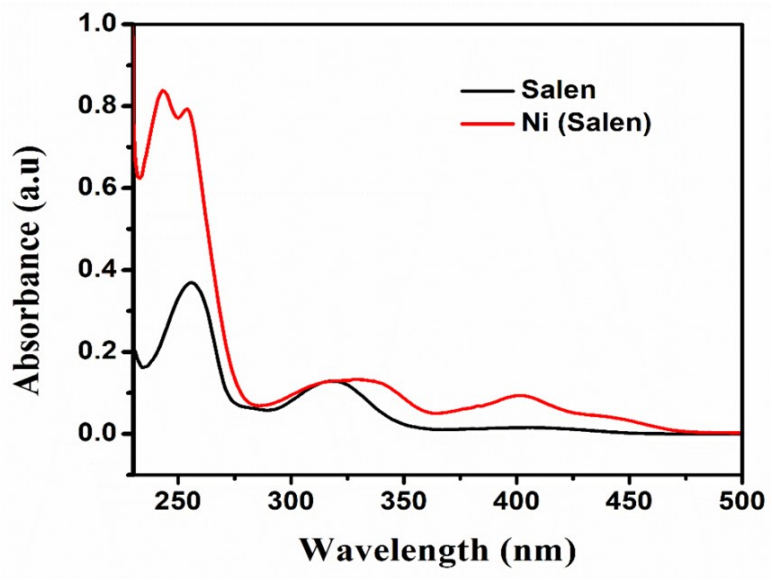

Figure S1. UV-Visible spectra of salen and Ni(salen) in acetonitrile solvent.

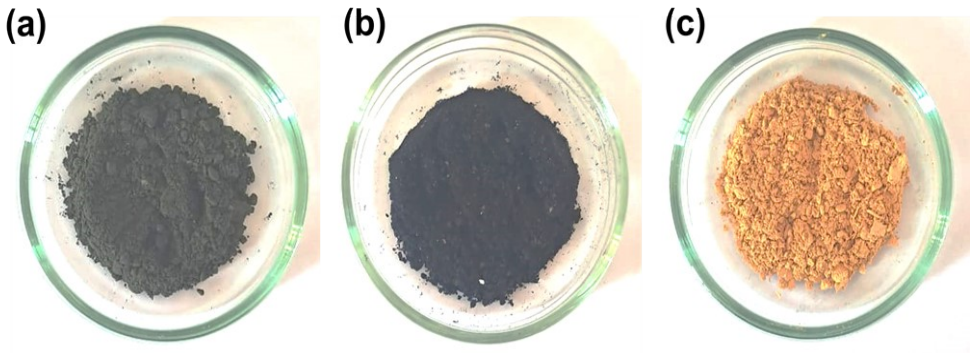

Figure S2. Photographic images of the synthesized precursors, (a) NVM-P (b) NV-P and (c) NM-P.

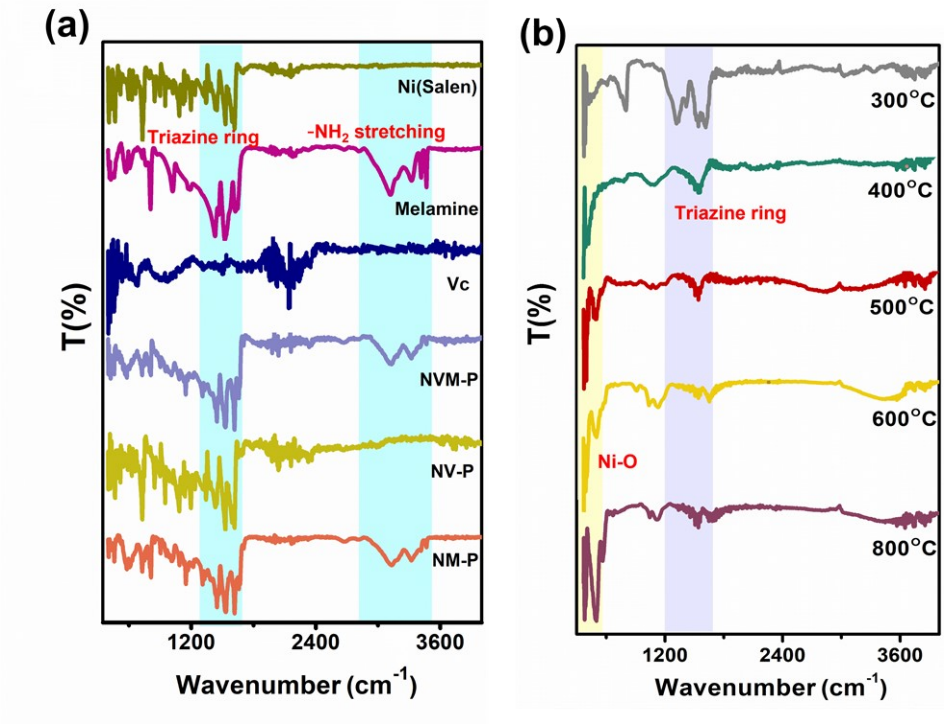

Figure S3. FTIR spectra of (a) Ni(salen), Melamine and Vc, along with their physical mixtures. (b) NVM-P samples subjected to thermal treatment at various temperatures.

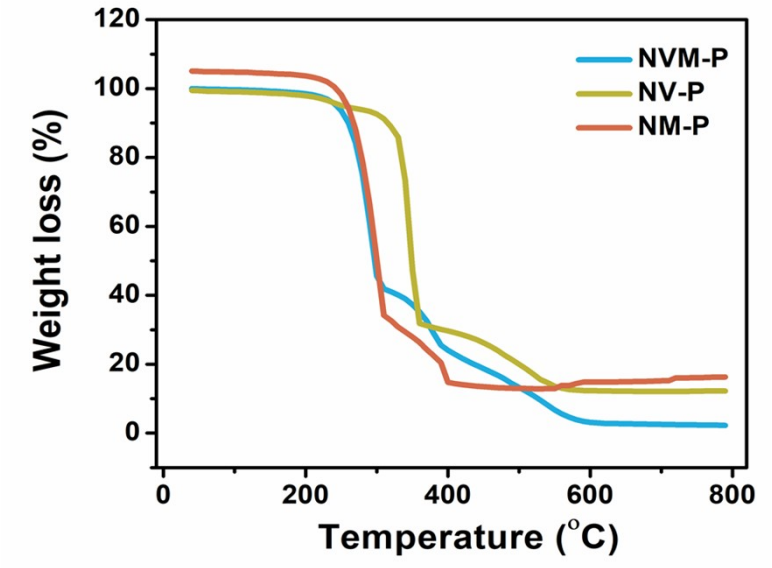

Figure S4. TGA spectra of the NVM precursors

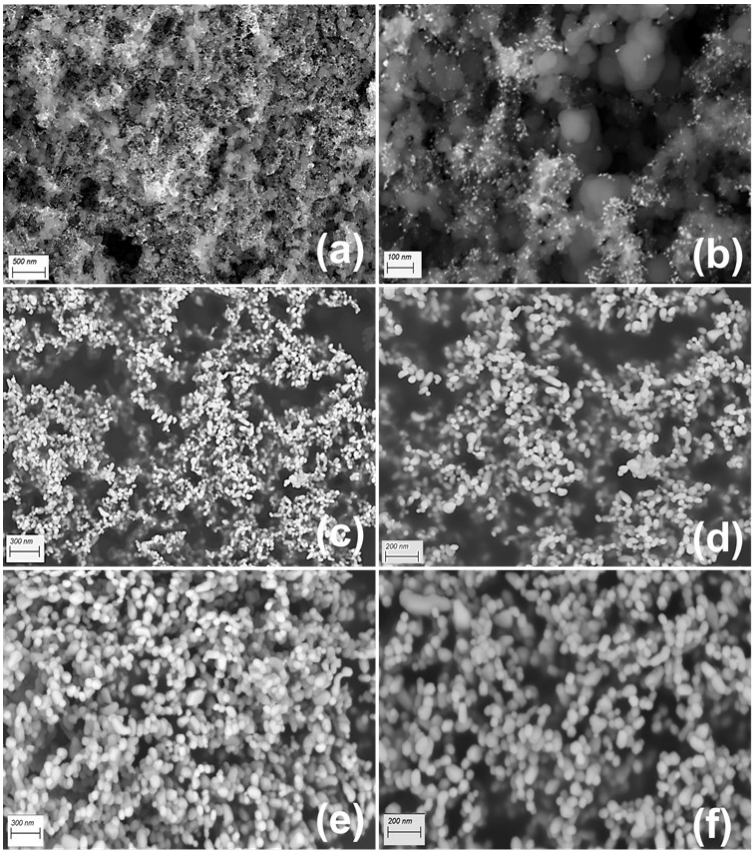

Figure S5. FESEM images of NVM-P samples heated at (a,b) 400 °C, (c,d) 600 °C, (e,f) 700 °C.

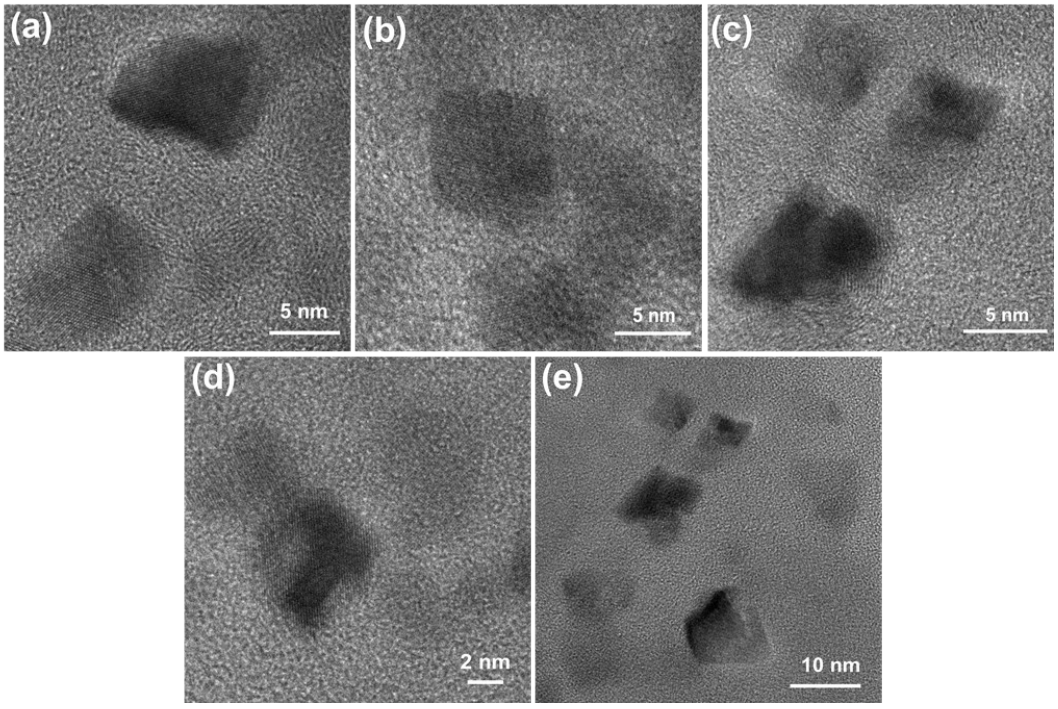

Figure S6. HRTEM images of NVM-P samples heated at 400 °C.

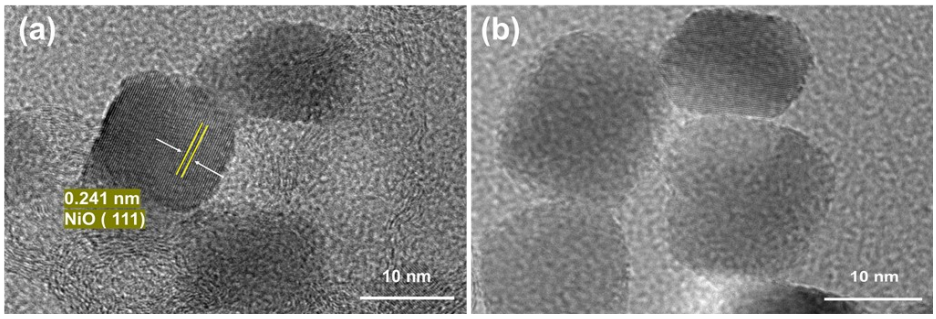

Figure S7. HRTEM images of NVM-P samples heated at 500 °C.

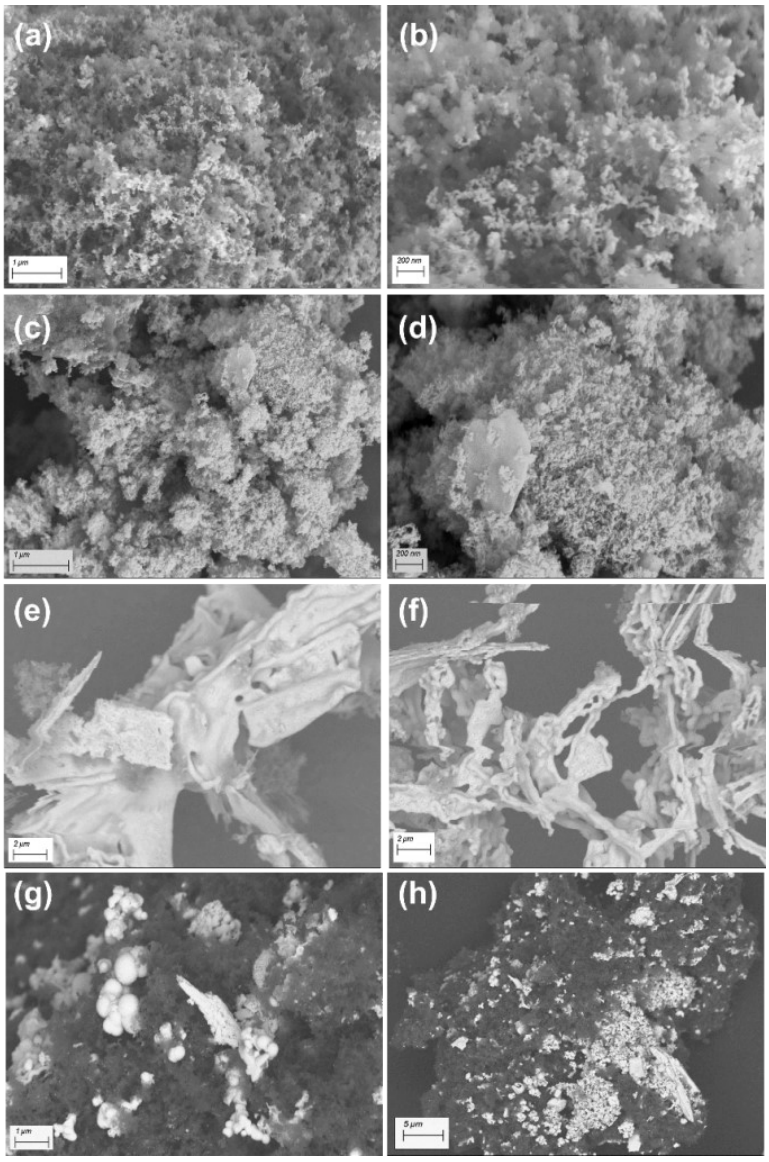

Figure S8. FESEM images of metal-salen complexes pyrolyzed at 500 °C: (a, b) Mn(salen), (c, d) Fe(salen), (e, f) Zn(salen), and (g, h) Sn(salen).

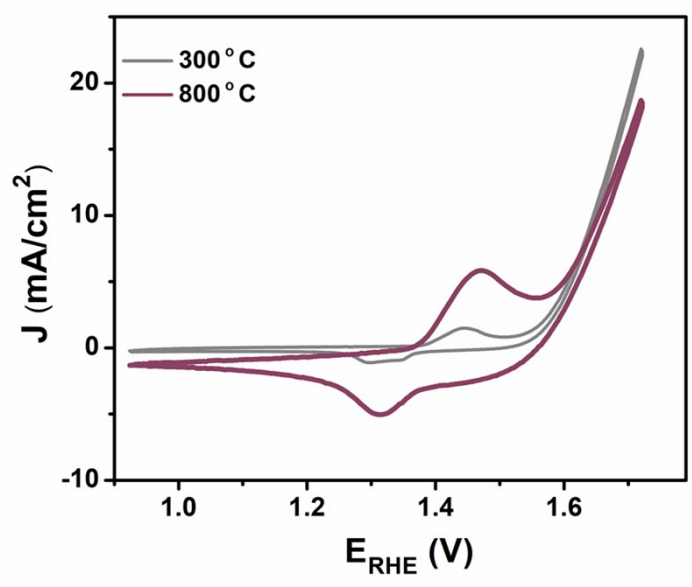

Figure S9. CV curves of NVM-P samples heated at various temperatures recorded in 1.0 M KOH electrolyte at a scan rate of 50 mV s^{-1},

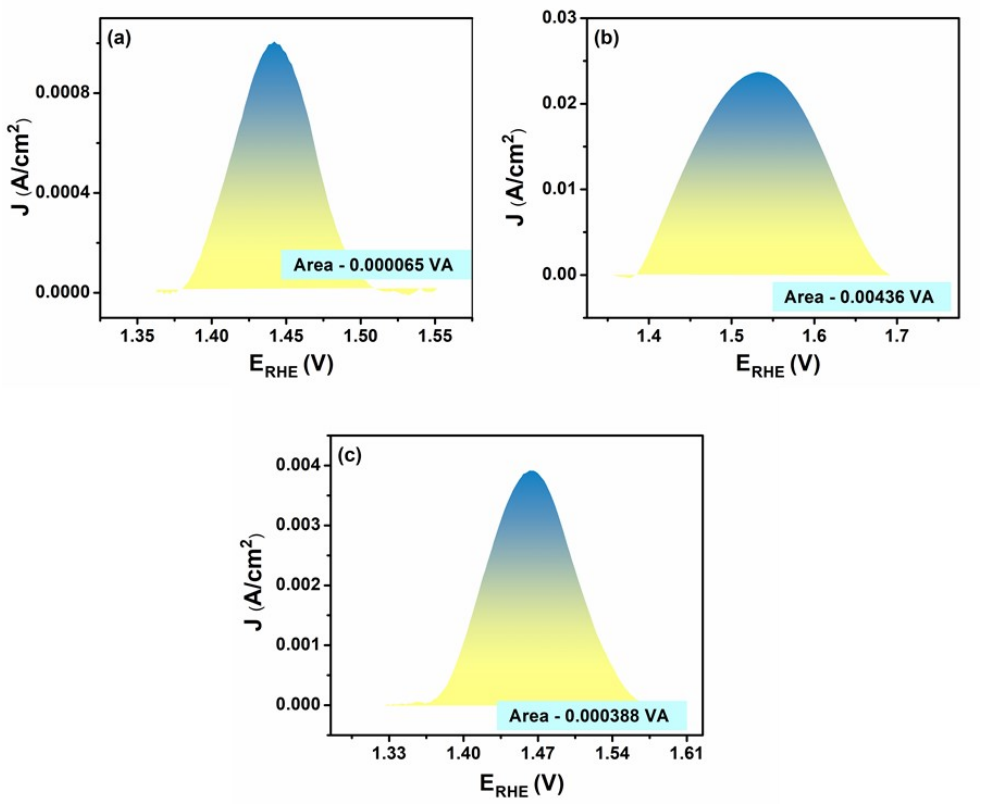

Figure S10. Area estimated from CV peak of (a) NVM-300 (b) NVM-500 (c) NVM-800 using the origin software to calculate the amount of electroactive Ni atoms.

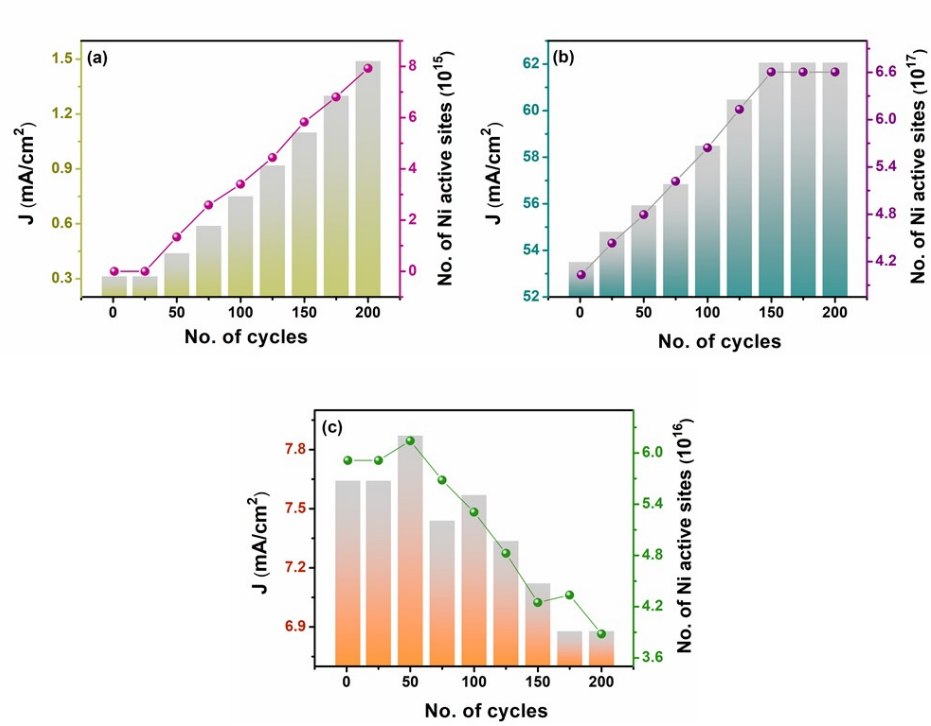

Figure S11. Anodic peak current and number of available active Ni sites as a function of cycle number for (a) NVM-300 (b) NVM-500 (c) NVM-800.

Note : 1

The charge associated with the Ni^{2+}/Ni^{3+} redox feature was obtained by numerical integration of the Faradaic peak in the current-potential curve and normalized to the scan rate to give the Faradaic charge per cycle. The normalization converts the area under the CV curve into the charge responsible for the redox process, which directly relates to the number of Ni active sites.

Reference : Roy, S. S.; Karmakar, A.; Madhu, R.; Nagappan, S.; Dhandapani, H. N.; Kundu, S. Three-Dimensional Sm-Doped NiCu-LDH on Ni Foam as Highly Robust Bi-functional Electrocatalyst for Total Water Splitting. ACS Appl. Energy Mater. ***2023****, 6 (8), 8818–8829 .*

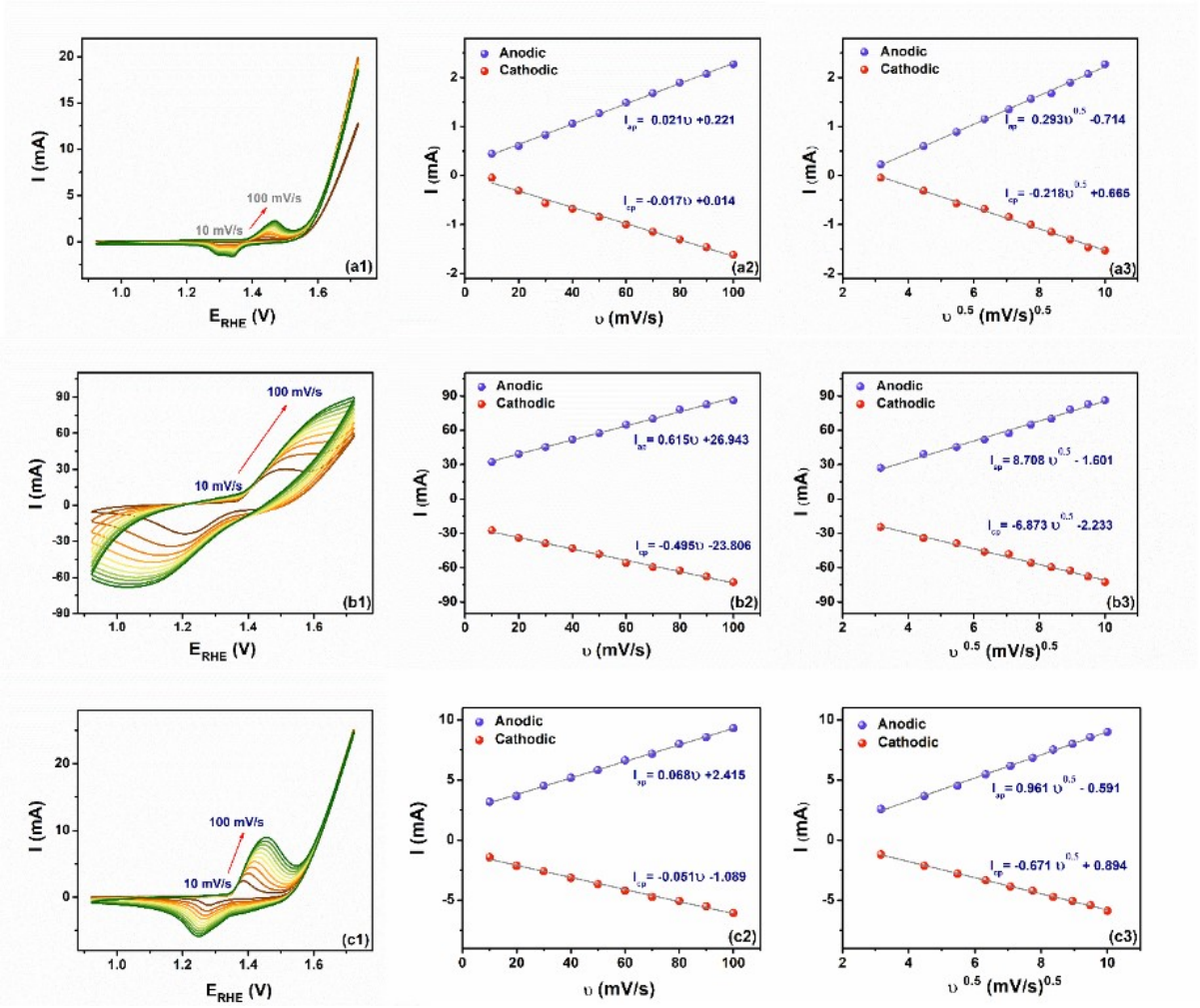

Figure S12. (a1-c1) CV curves of NVM-300, NVM-500, NVM-800 respectively in 1.0 M KOH at increasing potential scan rates (10, 20, 30, 40, 50, 60, 70, 80, 90 and 100 mV.s^{-1}), (a2-c2) relationship between anodic and cathodic current densities and the scan rates, (a3-c3) linear fitting of the anodic and cathodic peak current densities to the square roots of the scan rates.

Note : 2

The electroactive surface coverage (Γ*) of the Ni^{2+}/Ni^{3+} redox couple in the NVM catalysts was estimated using the following relation:

$$I_p = \left(\frac{n^2F^2}{4RT}\right)Av\Gamma^*$$

Here, I_p is the peak current, n represents the number of electrons transferred, F is the Faraday constant (96,845 C mol^{-2}), R is the universal gas constant (8.314 J K^{-1} mol^{-1}), T is the

temperature (298 K), v is the potential scan rate, and A is the geometric area of the glassy carbon electrode (0.09 cm^2). The values of Γ* were obtained from the slopes of the linear plots of I_p versus scan rate, averaged over both anodic and cathodic processes (Figure S8) .

The proton diffusion coefficient (D) at 298 K was further derived from the Randles -Sevcik equation:

$$I_p = 2.69 * 10^5 n^{\frac{3}{2}} A D^{\frac{1}{2}} C v^{\frac{1}{2}}$$

In this equation, I_p denotes the peak current, n the number of transferred electrons, A the electrode area, D the diffusion coefficient, C the initial concentration of electroactive species, and v the scan rate. Considering the density of $Ni(OH)_2$ (3.97 g cm^{-3}), the concentration of active species was approximated as 0.043 mol cm^{-3}.

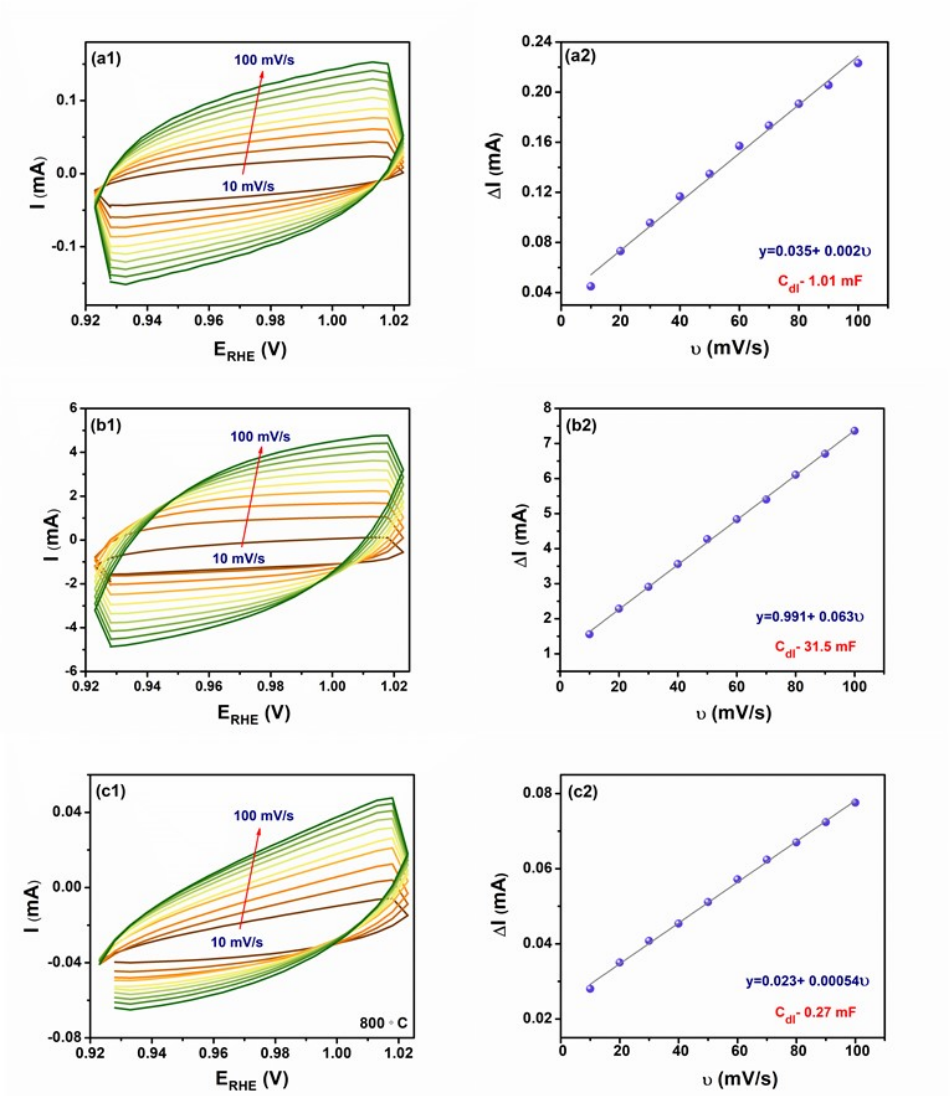

Figure S13. CV curves of NVM-300 (a1), NVM-500 (b1), and NVM-800 (c1), measured in the non-faradaic region in 1.0 M KOH at increasing potential scan rates (10, 20, 30, 40, 50, 60, 70, 80, 90, 100 mV s^{-1}). (a2-c2) displays the plots of linear relationship between anodic and cathodic charging current vs the scan rates at 0.97 V (RHE).

Note 3 :

The electrochemically active surface area (ECSA) of the synthesized catalysts was evaluated from the ratio of the double-layer capacitance (Cdl) to the specific capacitance (Cs) of the system. While Cs is regarded as a constant for a given electrolyte/electrode interface with a value of 0.40 mF cm^{-2}, Cdl was experimentally obtained from cyclic voltammetry (CV) measurements. For this purpose, CV scans were carried out at different scan rates within the non-Faradaic region (0.9–1.1 V vs. RHE). The resulting plots of current density (I) versus

scan rate (v) exhibited a linear dependence, with the slope corresponding to Cdl(Figure S9). Finally, the ECSA of each catalyst was determined according to the relation:

$$ECSA = \frac{Cdl}{Cs}$$

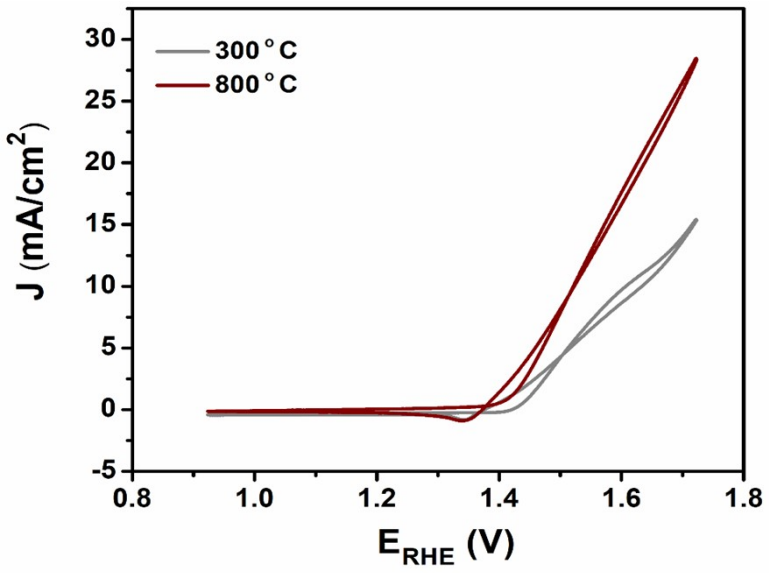

Figure S14. CV curves of NVM-P samples heated at various temperatures recorded in 1.0 M KOH electrolyte with 1.0 M CH_3OH solution at a scan rate of 50 mV s^{-1} .

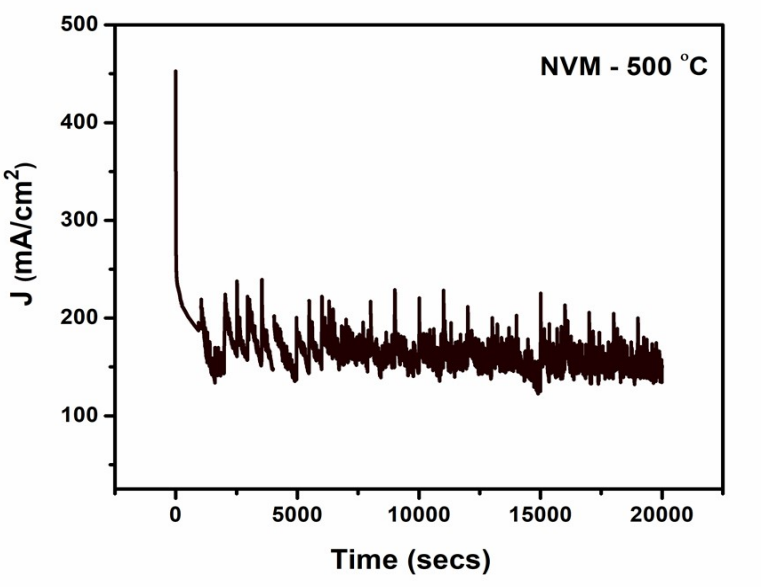

Figure S15. CA measurements were performed for NVM-500 sample in 1.0 M KOH at constant potential of 1.5 V.

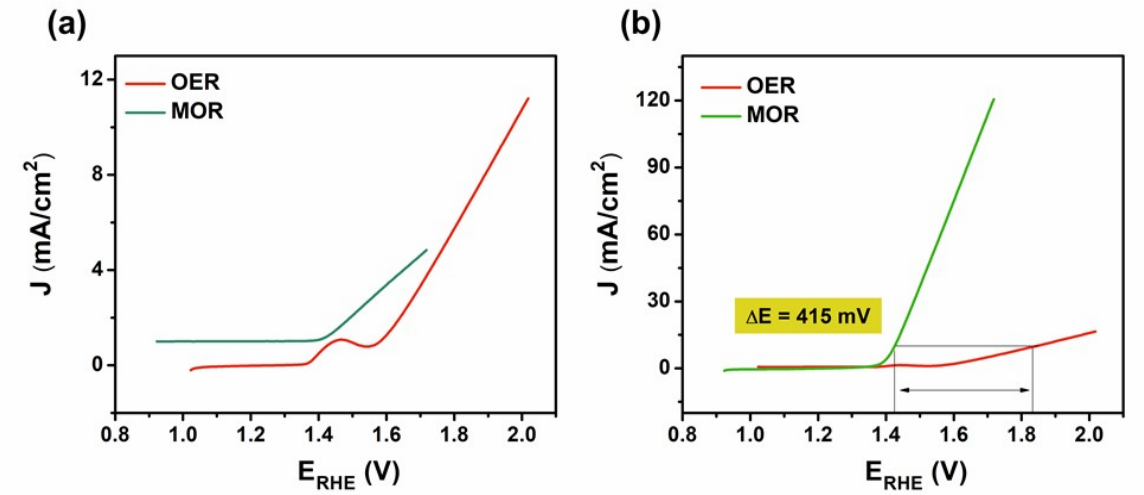

Figure S16. LSV curves of NVM-P samples heated at various temperatures recorded in 1.0 M KOH electrolyte with 1.0 M CH_3OH solution at a scan rate of 50 mV s^{-1}. (a) NVM-300 in 1.0 M KOH in the absence (OER) and presence of 1.0 M CH_3OH (MOR) (b) shows NVM-800 with a ΔE of 415 mV at 10 mA cm^{-2}.

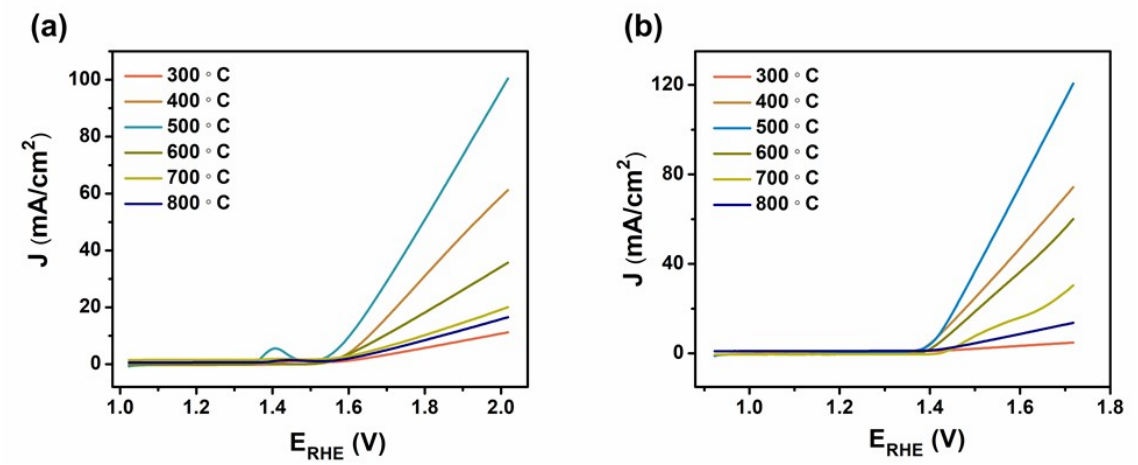

Figure S17. The LSV curves NVM electrodes in 1.0 M KOH (a) and 1.0 M KOH with 1.0 M CH_3OH solution (b), respectively at a scan rate of 5 mV s^{-1}.

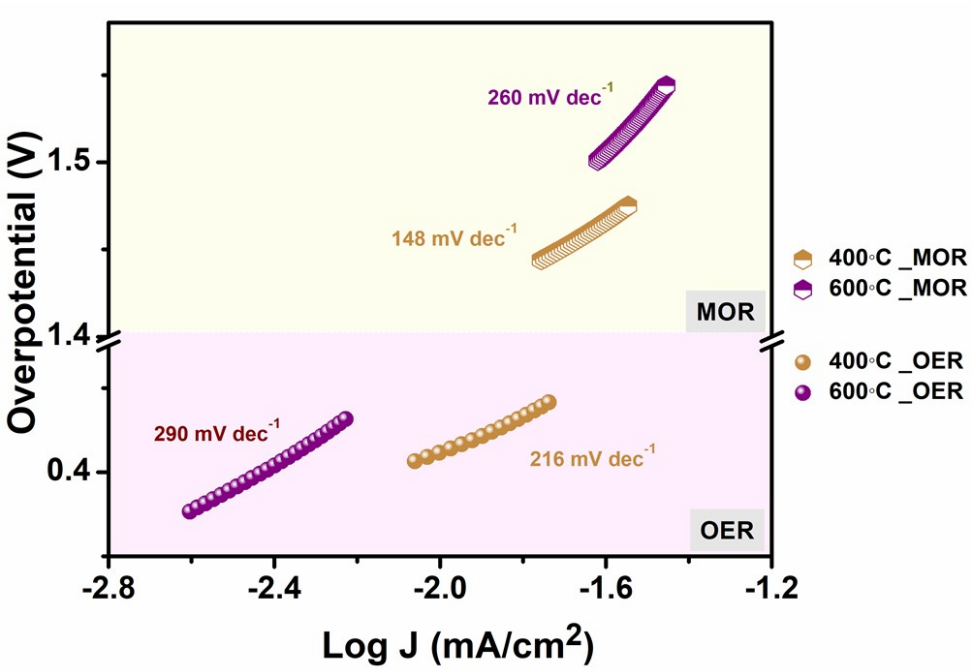

Figure S18. Tafel slopes of NVM electrodes for OER and MOR.